JOURNAL OF GEOPHYSICAL RESEARCH, VOL. 111, D23209, doi:10.1029/2006JD007278, 2006

Measurements of atmospheric parameters during Indian Space Research Organization Geosphere Biosphere Programme Land Campaign II at a typical location in the Ganga basin: 1. Physical and optical properties

S. N. Tripathi,[1] Vinod Tare,[1] N. Chinnam,[1] A. K. Srivastava,[1] Sagnik Dey,[1] A. Agarwal,[1] S. Kishore,[1] R. B. Lal,[1] Manish Manar,[1] Vijay P. Kanwade,[1] S. S. S. Chauhan,[1] M. Sharma,[1] R. R. Reddy,[2] K. Rama Gopal,[2] K. Narasimhulu,[2] L. Siva Sankara Reddy,[2] Shilpy Gupta,[3] and Shyam Lal[3]

Received 9 March 2006; revised 9 July 2006; accepted 18 August 2006; published 14 December 2006.

[1] This paper attempts to characterize the physical and optical properties of the aerosols along with relevant meteorological parameters at a typical location in the Ganga basin. The emphasis is on delineating the prolonged foggy/hazy conditions, a phenomenon believed to be of relatively recent origin, faced by millions of people during the winter months of December and January. Collocated measurements of a number of aerosol and atmospheric parameters were made using ground-based instruments as part of an intense field campaign launched under the Indian Space Research Organization Geosphere Biosphere Programme in December 2004. The meteorological conditions suggest limited mixing due to shallow boundary layer thickness and essentially calm wind conditions. Monthly mean aerosol optical depth was high (0.77 ± 0.3 at 0.5 μm wavelength) and showed high spectral variation (first-order Ångström exponent for all wavelengths, $\alpha = 1.24 \pm 0.24$). The second-order Ångström exponent α' derived for 0.34, 0.5, and 1.02 μm wavelengths showed much higher curvature in the aerosol optical depth spectrum on the hazy/foggy days (0.93 ± 0.36) as compared to that during the clear days (0.59 ± 0.3). Single-scattering albedo (0.87–0.97) showed strong spectral variation. Aerosol mass concentration was high with monthly average 125.9 ± 47.1 μg m^{-3}. Fine mode particles (<1 μm) contributed ~75% to the total mass of aerosols. Similarly, aerosol number concentration was found to vary in the range $1.5–2 \times 10^3$ cm^{-3}, with fine mode particles contributing to ~99.6%. The hazy/foggy conditions typically prevailed when higher daytime relative humidity, lower maximum temperature, and higher fine/accumulation mode particles were observed. The companion paper suggests that the rise in aerosol mass/number concentration could be attributed to the aqueous-phase heterogeneous reactions mediated by anthropogenic pollutants and the associated reduction in boundary layer thickness and suppressed mixing.

Citation: Tripathi, S. N., et al. (2006), Measurements of atmospheric parameters during Indian Space Research Organization Geosphere Biosphere Programme Land Campaign II at a typical location in the Ganga basin: 1. Physical and optical properties, *J. Geophys. Res.*, *111*, D23209, doi:10.1029/2006JD007278.

1. Introduction

[2] Some parts of northern India, particularly plains of the Ganges basin, are experiencing colder winters with prolonged and enhanced foggy/hazy conditions over the last decade. On the other side, the extreme dry and hot periods seem to be shrinking while the onset of sultry conditions appears to be advancing during the summers. Rapid increase in population, urbanization and industrial growth has resulted in increase of anthropogenic aerosol loading in the last few decades. The enormously high aerosol loading over the Ganga basin has been reported on the basis of satellite [*Goloub et al.*, 2001; *Chu et al.*, 2003; *Girolamo et al.*, 2004; *Ramanathan and Ramana*, 2005] and ground-based observations [*Mönkkonen et al.*, 2004; *Singh et al.*, 2004; *Dey et al.*, 2005]. Long-term measurements by the Central Pollution Control Board (CPCB), India, have revealed very high annual average concentrations (>150 μg m^{-3}, critical range according to the air quality standard in India) of

[1] Department of Civil Engineering, Indian Institute of Technology, Kanpur, India.
[2] Department of Physics, Sri Krishnadevaraya University, Anantapur, India.
[3] Physical Research Laboratory, Ahmedabad, India.

0148-0227/06/2006JD007278$09.00

particulate matter of diameter less than 10 μm (PM_{10}) in the atmosphere of the major cities of the Ganges basin (CPCB site, http://www.cpcb.nic.in). For example, in Kanpur, the average PM_{10} concentration in the last 5 years has been reported at 202 ± 73.1 μg m^{-3}.

[3] Over the last decade or so, a large number of researches have been directed to understand the climatic effects of atmospheric aerosols [*Hobbs et al.*, 1997; *Penner et al.*, 2001]. The effect of aerosols on climate is very complex and depends on several aerosol microphysical properties, such as composition, size distribution, hygroscopic behavior and other properties [*Jacobson*, 2001]. Aerosols influence the forcing indirectly through well-known Twomey effect [*Twomey*, 1977] and absorbing aerosols evaporate clouds thus affecting the hydrological cycle [*Ackerman et al.*, 2000; *Ramanathan et al.*, 2001]. Radiative forcing by aerosols is one of the largest sources of uncertainty in projecting climate change [*Charlson et al.*, 1992; *Kiehl and Briegleb*, 1993; *Satheesh and Ramanathan*, 2000; *Intergovernmental Panel on Climate Change*, 2001] because of the incomplete knowledge of the macrophysical and microphysical [*Dubovik et al.*, 2000, 2002] properties of aerosols. Therefore collation of information on chemical, microphysical and optical properties of aerosols, which are main inputs to the radiative forcing calculations, is warranted.

[4] Several international multi-institutional campaigns have been conducted in the past to understand the role of aerosols in climate change. The primary goal of the Aerosol Characterization Experiment (ACE) was to minimize the uncertainty in the estimation of aerosol radiative forcing in the clean Southern Hemisphere marine atmosphere during ACE 1 [*Bates et al.*, 1998] and subtropical northeast Atlantic during ACE 2 [*Raes et al.*, 2000]. Later on, similar campaign was conducted in the East Asian region (ACE-Asia) to understand these issues more comprehensively [*Huebert et al.*, 2003]. Smoke, Cloud, Aerosols, Radiation–Brazil (SCAR-B) was aimed at understanding the effect of biomass-burning aerosols and smoke on the forcing [*Kaufman et al.*, 1998]. Similar effort was made over the United States during Tropospheric Aerosol Radiative Forcing Observational Experiment (TARFOX) [*Russell et al.*, 1999]. In Europe, the ESCOMPTE program was conducted to create relevant database to produce regional pollution models [*Cros et al.*, 2004]. The Indian Ocean Experiment (INDOEX) was focused at the tropical Indian Ocean during the Northern Hemisphere dry monsoon, when the anthropogenic pollution was transported from the continent to the oceanic region. Till early 2004, no such exercise has been conducted on a large scale on the Indian subcontinent, which is necessary in order to understand the regional pollution dynamics, its transport to the oceanic region and effect on the climate. During February 2004, a mobile pilot land aerosol campaign was organized under Indian Space Research Organization Geosphere Biosphere Programme (ISRO-GBP) in southern India [*Moorthy et al.*, 2005a].

[5] In December 2004/January 2005 a monthlong land campaign with a multi-institutional scientific effort aiming to understand the pollution dynamics of the Ganga basin in northern India during winter season was carried out by ISRO (ISRO-GBP Land Campaign II). IIT Kanpur (longitude 80°22′E and latitude 26°26′N and 142 m altitude from mean sea level) was one of the 7 stations in the Ganga basin, where simultaneous measurements of optical, physical and chemical properties of aerosols were conducted during Land Campaign II (LC II).

[6] The principal goal of the research work presented in this and the companion paper was to test the hypothesis that anthropogenic aerosol loading significantly contributes to the prolonged and enhanced foggy/hazy winters in plains of the Ganges basin. Collocated measurements of particle mass, particle number size distributions, aerosol optical properties, e.g., aerosol optical depth (AOD), Ångström exponent α, single-scattering albedo (SSA) measured by sun/sky radiometer, were carried out. Such extensive simultaneous measurements are not reported in the literature for this region. Direct measurements of all the aerosol parameters reduce the uncertainties in the regional aerosol model, and hence are important to further the state of the art on role of aerosols in influencing atmospheric conditions.

2. Methodology

[7] ISRO-GBP LC II was conducted during 1–31 December 2004 continuously, when measurements of physical, optical and chemical properties of aerosols have been taken in stationary mode. During the campaign period, detailed measurements of aerosol parameters and trace gases were carried out at three sites, Delhi, IIT Kanpur and Kharagpur (Figure 1) out of the seven stations. At IIT Kanpur, measurements of some parameters were extended for another week.

[8] The primary objectives of the LC II were as follows: (1) to measure the physical, optical and chemical properties of the aerosols simultaneously, so that these properties can be used to estimate the aerosol radiative forcing more accurately; (2) to compare the properties of aerosol and trace gases in foggy/hazy and clear weather condition; and (3) to understand the fog chemistry in the northern India. During the winter season, mainly in December and January, the whole part of the Northern India experiences western disturbances moving eastward from west, which leads to intense fog and haze in the region [*Pasricha et al.*, 2003]. This is represented in Figure 1 using Moderate Resolution Imaging Spectroradiometer RGB image. Size-resolved fog water samples were collected and chemically analyzed using a fog sampler. The chemical composition of fog and its characteristics is subject of another paper.

[9] At IIT Kanpur, measurements were conducted using ground-based instruments, balloonsonde and aircraft to gather a comprehensive data set to understand the regional pollution dynamics and its effect on the radiation budget. The information about the boundary layer characteristics was obtained through balloon sonding. Vertical distribution of black carbon (BC) aerosols was measured using AE-21-ER Aethalometer on board an unpressurized high-wing Piper Super Cub PA-18 aircraft [*Tripathi et al.*, 2005b]. Continuous surface measurements of BC, its diurnal behavior and the implication to regional radiative forcing are discussed in details elsewhere [*Tripathi et al.*, 2005a].

[10] All the measurements have been performed following a common protocol, as the measurement sites were located at varying geographical locations and the measure-

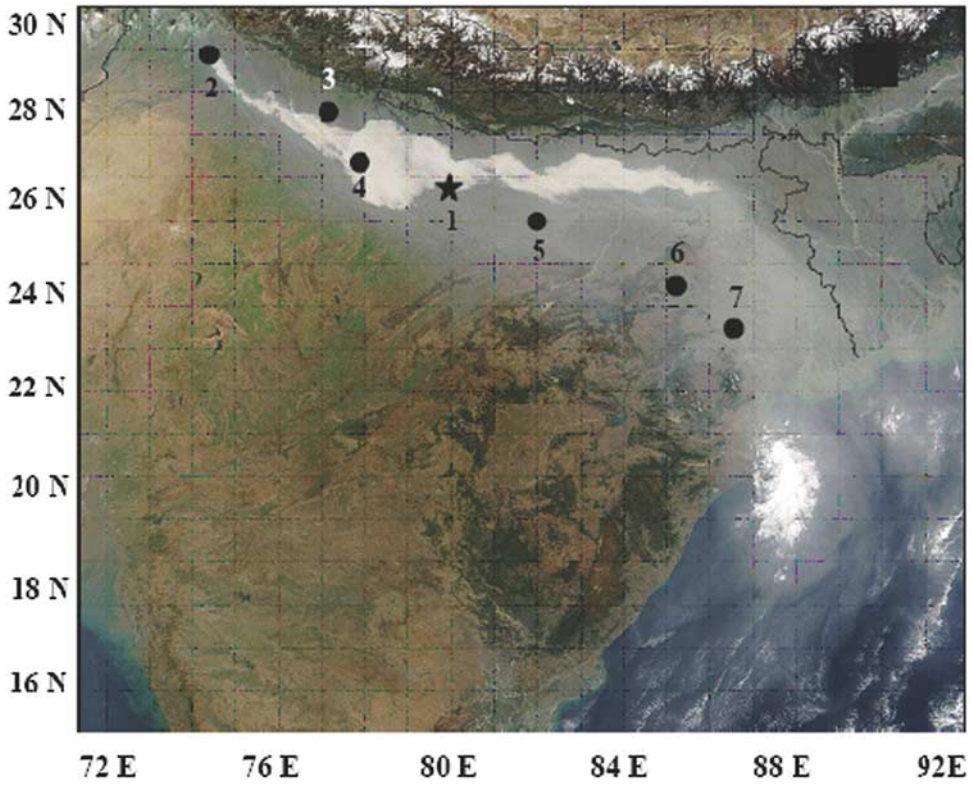

Figure 1. MODIS RGB image taken on board Aqua satellite on 18 December 2004 showing intense fog and haze spreading over the entire Ganga basin. The locations of Kanpur (1) and the other sites (2–7 represent Hissar, Delhi, Agra, Allahabad, Jaduguda, and Kharagpur, respectively), where simultaneous measurements were taken during LC II, are also shown.

ments were being taken by different individuals. The time window for the measurements was fixed from 0900 to 1700 local time (LT), as during this time period, the boundary layer is well evolved. The aerosol optical and physical properties were measured within this time zone, whereas BC measurements were taken continuously for 24 hours. Aerosol samples were collected during the specified time range; however, on some days, 24-hour samples were also collected to study the diurnal variations of the chemical composition of aerosols.

[11] A number of instruments were used to measure various aerosol parameters during the campaign (refer to Table 1). A brief description of the instrumentation and protocol for the measurement of the optical and physical parameters is given as follows.

2.1. Measurements of Meteorological Parameters

[12] During the campaign, the meteorological parameters (wind speed, WS; temperature, T; relative humidity, RH and precipitation) were measured by an automatic weather station of Envirotech Pvt. Ltd., New Delhi. The WS and T sensors work with an accuracy of 0.36 km hr^{-1} and 0.1°C, while the accuracy of RH sensor is 2% for RH < 90% and 3% for RH in the range of 90–100%. The measurements were taken in every 5 min. and the data are grouped and displayed as hourly average. Wind direction (WD) data at the surface and at ~300 m height from mean sea level were obtained from Chakeri air field, around 25 km away from IIT Kanpur. The WD data at the surface were recorded at an hourly interval, whereas the data at ~300 m height were taken by balloon measurements once in the morning and afternoon.

2.2. Measurements of Optical Properties

[13] Optical properties of aerosols were measured using CIMEL sun/sky radiometer deployed under the Aerosol Robotic Network (AERONET) program along with the

Table 1. Instrumentation and the Parameters Measured During Land Campaign II at Kanpur

Serial Number	Parameters	Instruments
1	AOD, water vapor	AERONET
2	AOD, water vapor	MWR
3	particle number distribution	GRIMM optical particle counter
4	particle mass distribution	quartz crystal microbalance
5	aerosol chemical composition	APM 450 Envirotech single-stage PM_{10} high-volume sampler, Pacwill Tisch Environmental Cascade impactor
6	fog water chemical composition	three-stage fog sampler
7	aerosol black carbon	aethalometer
9	Ozone	Microtops

multiwavelength radiometer (MWR) deployed under ISRO-GBP. The CIMEL radiometer takes measurements of the direct sun and diffuse sky radiances within the spectral range 0.34–1.02 μm [*Holben et al.*, 1998, 2001]. The direct sun measurements are made at eight spectral channels (0.34, 0.38, 0.44, 0.5, 0.67, 0.87, 0.94 and 1.02 μm) with triplet observations per wavelength and sky measurements at four spectral channels (0.44, 0.67, 0.87 and 1.02 μm) to deduce aerosol optical properties. AOD due to fine and coarse mode are discriminated following *O'Neill et al.* [2003], which further help in assessing the anthropogenic contribution. The optical properties are measured both at fine (<1 μm) and coarse (>1 μm) modes. The uncertainty in calculation of aerosol optical depth (AOD) and error analysis of retrieved optical properties, e.g., SSA and volume size distribution, are given in detail by *Dubovik et al.* [2000]. Level 2.0 data of AERONET are used in the present study.

[14] MWR provides AOD by measuring continuous spectral extinction measurement of direct solar radiation at ten narrow spectral filters at 0.38, 0.4, 0.45, 0.5, 0.6, 0.65, 0.75, 0.85, 0.935 and 1.025 μm wavelength [*Moorthy et al.*, 1999]. Each set of MWR observation is composed of measurement time and output voltage. From the voltage measurements, AOD is obtained using Langley plot technique, details of which are given by *Moorthy et al.* [1999].

[15] The AOD retrieved by AERONET and MWR are in excellent agreement ($R^2 \sim 0.96$) during the winter season in the region with maximum absolute difference of 0.06 (K. K. Moorthy et al., private communication, 2004). Hence, during the absence of the CIMEL radiometer due to a technical problem in December 2004, AOD data were complemented from the MWR to create a continuous database for the whole month. During the time of intense fog, AOD could not be measured because of the absence of direct sunlight. First-order Ångström exponent (α) is computed from the spectral variation of AOD in the wavelength range 0.34–1.02 μm using the *Ångström* [1964] relationship:

$$\tau_a = \beta\lambda^{-\alpha} \tag{1}$$

where β is the turbidity coefficient and λ is the wavelength. Further, a second-order Ångström exponent (α') has been derived following *Eck et al.* [1999] to quantify the rate of change of slope in $\ln \tau_a - \ln \lambda$ curves:

$$\alpha'(\lambda) = \left(\frac{-2}{\ln\lambda_{i+1} - \ln\lambda_{i-1}}\right)\left(\frac{\ln\tau_{a_{i+1}} - \ln\tau_{a_i}}{\ln\lambda_{i+1} - \ln\lambda_i} - \frac{\ln\tau_{a_i} - \ln_{a_{i-1}}}{\ln\lambda_i - \ln\lambda_{i-1}}\right). \tag{2}$$

In this study, we calculated α' using 0.34, 0.5 and 1.02 μm wavelengths to cover the wavelength spectrum used by AERONET. α' close to zero indicates constant slope of the AOD spectrum, while a higher value represents rapidly changing slope. Aerosol volume size distribution is retrieved in the particle size range 0.05–15 μm with insignificant error in the range 0.1–7 μm [*Dubovik et al.*, 2000].

2.3. Physical Measurements

[16] Total ambient aerosol mass concentration (M_T) was measured, using a quartz crystal microbalance (QCM, model PC-2 of California measurements), with the accuracy of about 15–20% for $M_T < 10$ μg m^{-3} [*Pillai and Moorthy*, 2001]. The error is even less for higher M_T. QCM is a Cascade impactor that has the potential to provide near-real-time measurements of total as well as size segregated mass concentration of aerosols. The impactor is provided with a small pump (diaphragm vacuum pump) to aspire the ambient air into the stack, and a flowmeter to monitor the flow rate. The instrument operates at a flow rate of 240 ml min^{-1} and segregates aerosol samples in the range 0.05 to > 25 μm in 10 size bins. The low flow rate was used, as only a very small amount of aerosol mass is required to produce a measurable frequency drift. Measurements were made approximately at hourly intervals from 0900 to 1700 LT for the whole month of December with the sampling duration of 6 min. The short-term stability of the crystal oscillator during the sampling time of 6 min is more important than long-term drift as M_T is directly proportional to the change in the frequency difference of the sensing and the reference crystal. The most important parameter that controls QCM's operation is RH. At RH > 70%, it requires stable RH during the sampling period [*Pillai and Moorthy*, 2001], because of the affinity of quartz substrate to moisture. Also, there could be the loss of adsorbed water from water-soluble particles by evaporation during the collection of particles under low-pressure conditions [*Jayaraman et al.*, 1998]. The maximum error in measured mass for high ambient RH could be ~25%. During the measurement period (0900–1700 LT), whenever ambient RH crosses 75%, the instrument operation was discontinued. During the foggy/hazy days, the crystals were regularly cleaned and dried, so that the moisture effect can be minimized. Thus enough precautions were taken during the data collection, but still, some error exists in the measured mass concentration, which arises because of the uncertainty in the assumed aerosol density (2 gm cm^{-3}; *Pillai and Moorthy* [2001]). Earlier QCM was successfully used in INDOEX [*Jayaraman et al.*, 1998] and ARMEX [*Moorthy et al.*, 2005b] campaigns to measure mass size distribution. During ARMEX campaign, QCM was operated at highly humid conditions, where RH was more than 65% for most of the times.

[17] The particle size analyzer/dust monitor Model 1.108 (Grimm, Germany), also known as optical particle counter (OPC) is a small portable unit, used for the continuous measurements of particles in the air (http://www.grimm-aerosol.com). This instrument enables real-time measurements of ambient aerosol number concentration under varying environmental conditions [*Tiwary and Colls*, 2004]. The measurements were carried out in number mode, i.e., particle counts as counts liter^{-1} with an operational flow rate of 1.2 liters min^{-1}. This instrument uses the laser scattering technology for single particle counts, whereby a semiconductor laser serves as the light source. The scattered signal from the particle passing through the laser beam and is collected at approximately 90° by a mirror and transferred to a recipient diode. The instrument measures the cumulative number concentration in 15 channels in the range 0.3 to 20 μm with a detection range in 1–10^6 counts liter^{-1} with a sensitivity of 1 particle liter^{-1}. Particle number distributions were measured continuously from 0900 to 1700 LT everyday according to the measurement protocol. The major limitation of the measurements with the above two instru-

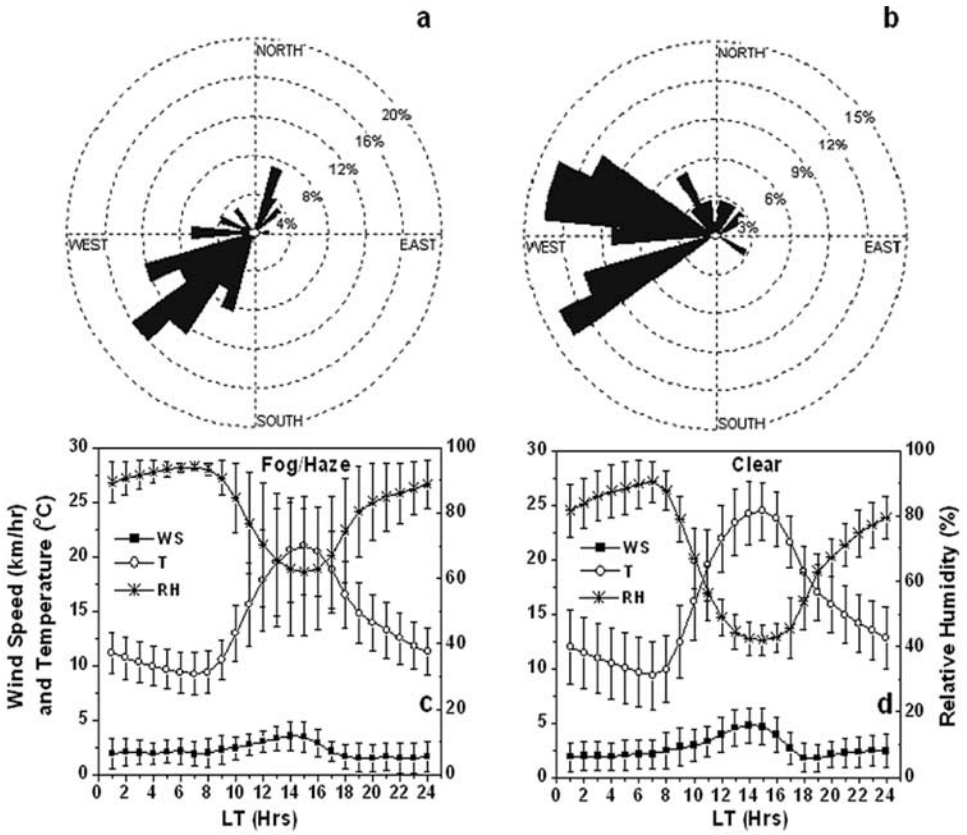

Figure 2. Wind direction (a) at the surface and (b) at 304.8 m altitude from mean sea level and diurnal variations of relative humidity (RH), wind speed (WS), and temperature (T) during (c) foggy/hazy and (d) clear days.

ments is that they cannot be operated during the haze when surface RH becomes higher than 75%; hence no nighttime measurements were possible during the campaign.

3. Results and Discussion

[18] The IITK campus is about 17 km away from the center of Kanpur City (shown in Figure 1) and is considered relatively free from local perturbations; hence it represents more regional characteristics than local nature. The main sources of particulate and gaseous pollutants from anthropogenic activities include biomass burning in open fields and as domestic fuel in rural settings [*Venkataraman et al.*, 2005], emissions from thermal power plants, brick kilns, fossil fuel burning and vehicular exhausts.

3.1. Synoptic Meteorology

[19] Foggy/hazy conditions were observed for significant number of hours on every day from the night of 8 December to the morning of 28 December (except on 25–26 December). Similar conditions prevailed during 4–5 January 2005. Accordingly, measurements conducted during 9–27 December (except 25–26 December) and 4–5 January were taken as representative of the foggy/hazy weather. The remaining measurements during the campaign period were considered to represent clear weather.

[20] The WD during the campaign was mostly southwesterly (Figure 2a) with occasional (~10%) northeasterly flow at the surface. Calm conditions were found to prevail near the surface frequently during the measurement period (~43%) leading to poor dispersal of the pollutants. At ~300 m altitude, the WD was mostly varying from northwesterly to southwesterly (Figure 2b). WS, RH and T show pronounced diurnal variations both during the foggy/hazy (Figure 2c) and clear (Figure 2d) weather conditions. WS was less than 2.5 km hr^{-1} during the early morning and nighttime, whereas the daytime WS was higher reaching ~4.0 km hr^{-1} at 1400 LT. The diurnal variation of the WS was almost similar during the foggy/hazy and clear weather conditions. RH was very high (>85%) during the nighttime and the early morning and decreased after 900 LT attaining a minimum value of 53% during the noontime. During the foggy/hazy weather days, RH never dipped below 70% (Figure 2c). The diurnal variation of T was lower during the foggy/hazy weather ($9°C < T < 18°C$) compared to clear weather days ($9°C < T < 24°C$). No precipitation was observed in December 2004; only a light drizzle was observed during the night of 2 January 2005. The absence of precipitation during the campaign rules out the wet removal processes of aerosols and provides a longer residence time in the atmosphere.

3.2. Atmospheric Stability and Boundary Layer

[21] Six balloon sondings were made in the morning hours (1000–1030 LT) during the campaign period. Temperature, relative humidity (RH), and potential temperature (θ) profiles obtained are presented in Figures 3a, 3b, and 3c,

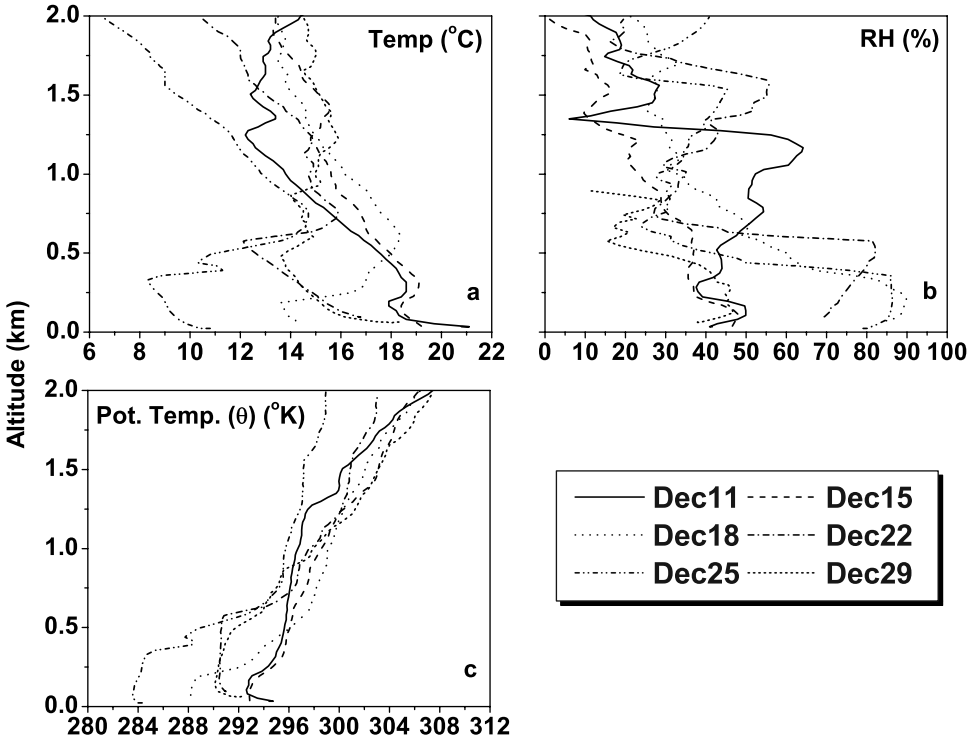

Figure 3. Vertical profiles of (a) temperature, (b) RH, and (c) potential temperature obtained from balloon soundings during December 2004.

respectively. The potential temperature (θ) is calculated from the following equation:

$$\theta = T_2[P_1/P_2]^{\kappa} \quad (3)$$

where $\kappa = R/c_p$; R is the specific gas constant for dry air and c_p is the specific heat capacity of dry air at constant pressure. Increasing θ with height (on 15, 18, and 25 December 2004) clearly indicates the presence of a stable layer near the surface during morning hours, which resembles the classical boundary layer structure during the morning hours in winter season [*Tripathi et al.*, 2005b]. For the rest of days (11, 22, and 29 December 2004) the inversion layer was found to be above 200 m altitude from surface. Because of this stable boundary layer, aerosols' mixing and dispersion are likely to be restricted. It may be noted that because of some technical problem in relative humidity sensor on 29 December, the data above 900 m were erroneous and hence not considered. Profiles of θ show the presence of stable layer except very near to surface (<200 m) where θ decreases with height with the enhanced mixing.

3.3. Aerosol Optical Properties

3.3.1. Aerosol Optical Depth Spectra

[22] Daily variations of AOD at 500 nm, $\tau_{a,500}$ along with α and α' are shown in Figure 4a, and their mean values during clear and hazy/foggy days are presented in Table 2. $\tau_{a,500}$ shows large variability from 0.35 to 1.6 during the period with monthly mean value of 0.77 ± 0.29. Variation in α values (1.23 ± 0.24) during December 2004 indicates high spectral variability in AOD. However, the monthly mean α appears to be underrepresented, as on few days, α was very low (<0.75). In fact on most of the days, α was higher than 0.9 indicating dominance of fine (nuclei and accumulation) mode particles. The backward trajectories of the air mass at 500, 1000 and 1500 m altitude calculated using archived FNL data of NOAA HYSPLIT model for 25 December 2004 (when $\alpha < 0.75$) show that the air mass at all three altitudes were transported from the western Thar Desert (Figure 4b). Hence it is quite likely that coarser dust particles carried away by the wind were added to the column along with local soil dust leading to such lower spectral variation of AOD. There is not much difference in the mean values of α during the clear and hazy/foggy days because of the sudden influx of coarse particles on 24–25 December, which lowers the mean of hazy/foggy period. If those two days are not considered, the mean becomes 1.4 ± 0.05, indicating higher spectral dependence due to higher fine mode particles, also noted from the AOD values.

[23] The slope of AOD spectrum on a log-log scale on most of the days is not constant, as revealed by α', which is not surprising for the urban aerosols [*Eck et al.*, 1999]. The monthly averaged AOD spectrum, when fitted linearly (slope of the line is α) on a log-log scale shows a difference of 0.08 and 0.047 at 0.34 and 0.5 μm wavelength, whereas, the corresponding differences in polynomial fit (required for derivation of α') are only 0.01 and 0.018, respectively. α' varies within a range of 0.15 (less curvature) to 1.53 (strong curvature) during the study period. During the hazy/foggy period, the mean value of α' was 0.93 ± 0.36, whereas, in the clear days, the mean value was 0.59 ± 0.3 (Table 2). This clearly indicates that the curvature in the AOD spectrum increases during the hazy/foggy days

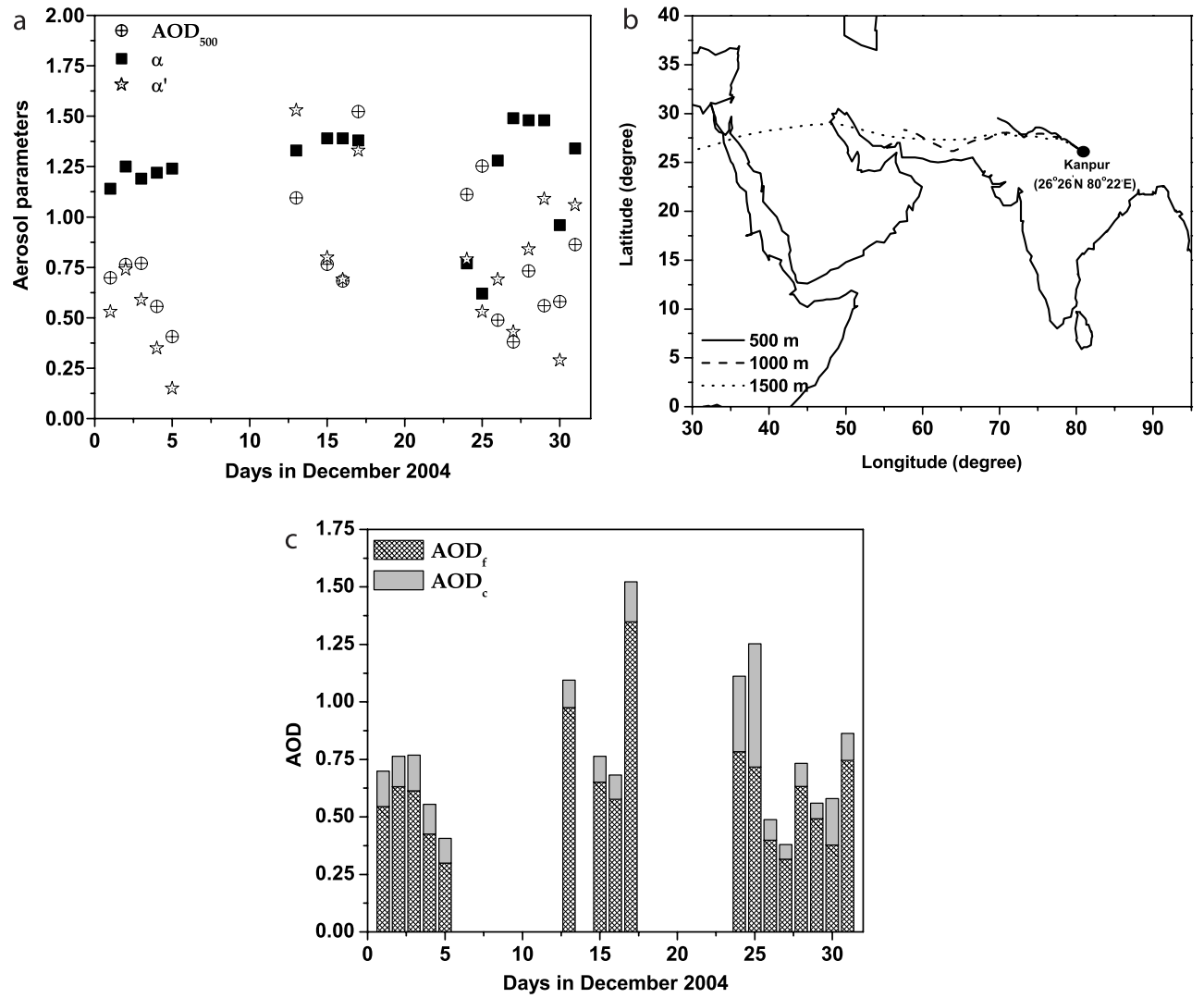

Figure 4. (a) Daily averaged AOD and first-order Ångström exponent α and second-order Ångström exponent α' during December 2004. (b) Five-day backward trajectories of the air mass at 500, 1000, and 1500 m altitude on 25 December. (c) Daily variation of AOD_f and AOD_c at 500 nm wavelength in December 2004.

because of increasing dominance of positive curvature in the accumulation mode aerosols.

[24] Further, to assess the role of anthropogenic activity in aerosol loading, fine mode AOD and coarse mode AOD are separated and presented in Figure 4c. The average fine mode AOD during the observation period is 0.62 ± 0.26, whereas the coarse mode AOD is 0.16 ± 0.11. The fine mode AOD increases from the monthly mean significantly (by 33%) during the hazy/foggy days, whereas, coarse mode AOD does not show so much increase. Only during 24 and 25 December, when α shows low values, coarse mode AOD was found to show threefold increase. Higher fine mode AOD during hazy/foggy condition indicates higher accumulation mode particle concentration (resulted from anthropogenic activities) and poor dispersal within the boundary layer. This fact is supported by the direct measurements of aerosol mass concentration by QCM, which is discussed in section 3.4.

3.3.2. Single-Scattering Albedo

[25] The temporal variations of SSA during the campaign at four AERONET retrieval wavelengths are shown in Figure 5a. SSA was found to vary in the range 0.87–0.97. *Dey et al.* [2005] have shown significant difference in SSA at fine and coarse mode in Kanpur during the winter season. However, here SSA retrieved for total size distribution is considered. Low values of SSA indicate presence of absorbing aerosols in significant amount in the region. During

Table 2. Aerosol Parameters During Foggy/Hazy and Clear-Sky Conditions

Sky Conditions	$AOD_{f,500}$	$AOD_{c,500}$	α	α'
Foggy/hazy	0.81 ± 0.27	0.21 ± 0.16	1.2 ± 0.35	0.93 ± 0.36
Clear	0.48 ± 0.15	0.12 ± 0.04	1.26 ± 0.15	0.59 ± 0.3

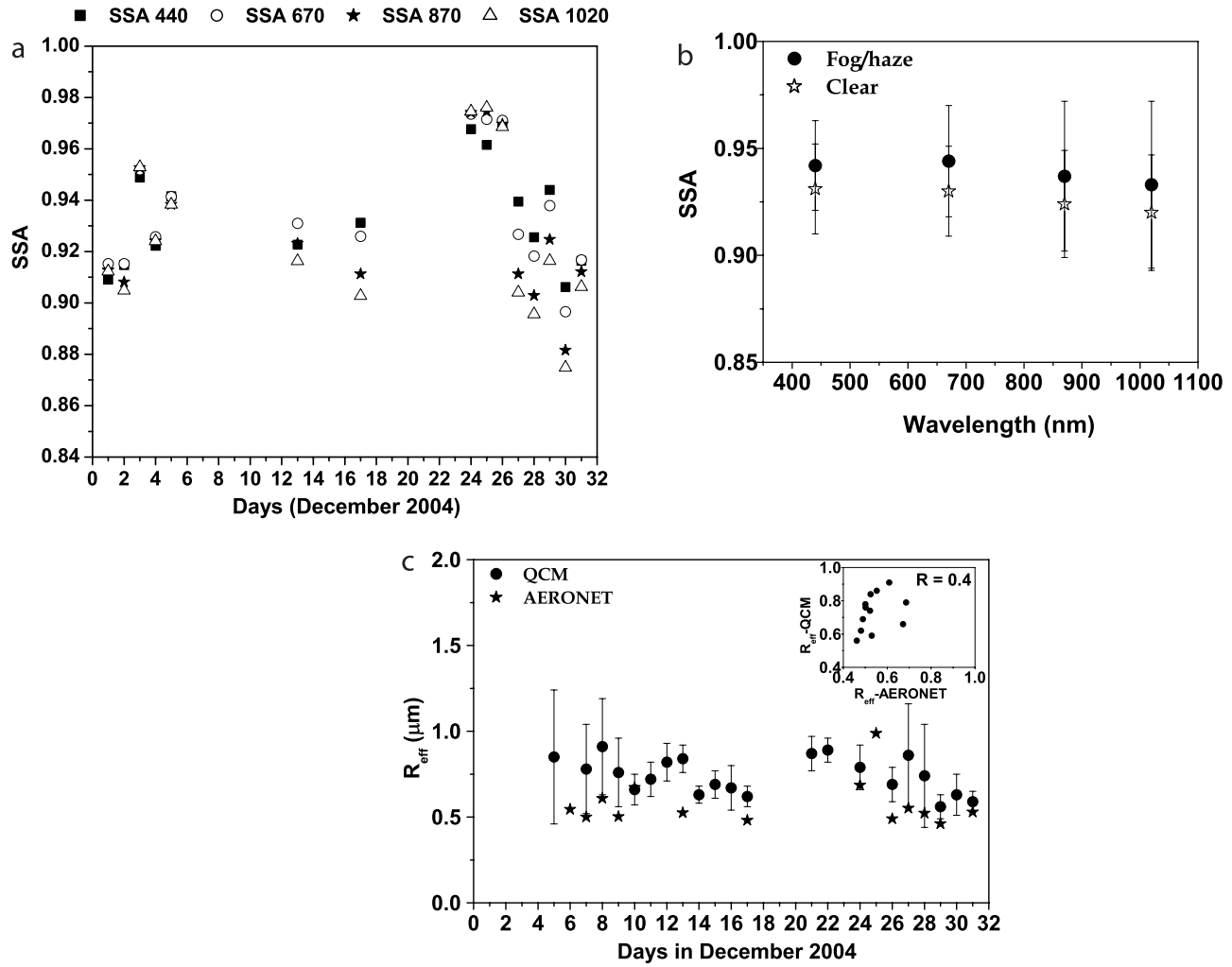

Figure 5. (a) Spectral variation of SSA during LC II retrieved from AERONET data. (b) Mean SSA spectra for foggy/hazy and clear days during the study period with standard deviation plotted as the error bars. (c) Daily averaged R_{eff} during the campaign period.

the campaign period, BC mass concentration was also measured, which is quite high in absolute terms (12.4 ± 0.5 μg m^{-3}) as well as mass fractions (~10%) [*Tripathi et al.*, 2005a; *Dey et al.*, 2006].

[26] SSA shows strong spectral dependence. SSA decreases with increase in wavelength for most of the days. *Bergstrom et al.* [2002] have shown that for $\alpha > 1$, the decreasing trend in SSA implies mixing of BC with non-absorbing components, which is very likely in Kanpur, where concentrations of scattering aerosols (e.g., sulfate, nitrate, etc.) are high (as reported in the companion paper, *Tare et al.* [2005]). This type of spectral variation of SSA arises from the fact that the rate of decrease in the scattering coefficient with wavelength is higher than that of absorbing coefficient. In the presence of larger particles, when $\alpha < 0.75$ (on 24 and 25 December), reverse trend in SSA was observed. The extinction coefficient of coarser dust particles does not show significant spectral variation; whereas, the absorption coefficient decreases with wavelength. Hence, in the presence of coarser particles, SSA (which is the ratio of scattering coefficient to the extinction coefficient) increases with wavelength. The spectral dependence of SSA during the clear and hazy/foggy days is shown in Figure 5b. At all four representative wavelengths, SSA is higher during the hazy/foggy days indicating higher concentration of scattering aerosols. This is quite obvious, as at high ambient RH in these days, scattering aerosols grow hygroscopically, as compared to the clear days. These SSA are of the ambient aerosols. We have linearly fitted the SSA with RH at each wavelength to estimate the SSA for dry aerosols ($\omega_{0,dry}$), and the results are summarized in Table 3. The intercepts of the best fit lines are taken as the $\omega_{0,dry}$ for that particular wavelength. The spectral dependence of $\omega_{0,dry}$ is higher than that of the ambient aerosols

Table 3. Relative Humidity Dependence of Single-Scattering Albedo During the Study Period in Kanpur

Wavelength, nm	$\Delta\omega_0/\Delta$RH	$\omega_{0,\ dry}$	Correlation Coefficient
440	0.0011	0.871	0.6
670	0.0014	0.854	0.68
870	0.0016	0.833	0.66
1020	0.0017	0.823	0.64

because of the higher rate of change of SSA with RH ($\Delta\omega_0/\Delta$RH) at higher wavelengths.

3.3.3. Aerosol Effective Radius

[27] The effective radius (R_{eff}) is a useful measure of average aerosol particle size in a polydisperse aerosol population. R_{eff} has been estimated from the QCM measurements using the formula:

$$R_{eff} = \frac{\sum_{i=2}^{10} V_{ci}}{\sum_{i=2}^{10} a_{ci}} \quad (4)$$

where V_{ci} and a_{ci} are the volume and area concentration of aerosols and they are summed over second to tenth stage of QCM. The first stage is excluded as it collects the particles having size more than 25 μm and no meaningful mean radius can be assigned to this stage [*Pillai and Moorthy*, 2001]. R_{eff} from each observation are averaged to obtain one value for each observation day. R_{eff} has been found to vary in the range 0.56 to 0.9 μm in the observation period. On 25 December, when sudden influx of coarse particles was observed, R_{eff}, as expected, showed the highest value (0.98 μm). Statistically, the mean for the clear days (0.71 ± 0.14) is not much different from the mean for hazy/foggy days (0.76 ± 0.1), but it is evident that during the hazy/foggy period, the diurnal variation (as represented by the standard deviations of each point plotted as error bars in Figure 5c) of R_{eff} is much lower compared to that during the clear days. During the hazy/foggy period, much stable atmosphere led to poor dispersal of the pollutants, resulting in less variation in the size distribution.

[28] R_{eff} has also been retrieved by AERONET and compared with R_{eff} estimated from QCM measurements (correlation coefficient of 0.4). Although R_{eff} from AERONET is lower as compared to that calculated from QCM measurements, the temporal trend is similar through out the observation period. The discrepancy in the values could be due to the fact that R_{eff} retrieved by AERONET is for the total atmospheric column, which may have slightly different size distribution than that at the surface, whereas the QCM-derived R_{eff} is for the near-surface aerosol size distribution. Also, in the QCM measurements, the first channel (particle >25 μm) is ignored for the derivation of R_{eff}. Another factor, that may be responsible for such discrepancy is RH. The mass concentration measured by QCM assumes particle density of 2 g cm^{-3}. At humid condition (mostly in the hazy/foggy period), hygroscopic growth of particles might lower aerosol density, which resulted in higher values of R_{eff}.

3.4. Physical Properties

3.4.1. Aerosol Mass Concentration

[29] Size-segregated aerosol mass concentration was measured using QCM. Total particle mass concentration (M_T), during the month of December, varied between 45 to 220 μg m^{-3} with a monthly mean of 126.0 ± 47.1 μg m^{-3}. Aerosols in Kanpur are mostly contributed by street dust and anthropogenic activities [*Dey et al.*, 2004; *Singh et al.*, 2004]; anthropogenic and industrial particles contributing to particle diameter $D_p < 2$ μm and dust contributing to $D_p > 2$ μm. M_T was divided into coarse mode (geometric mean diameter, D_p = 1.13 μm, this was done because 1.13 μm was the nearest D_p, which is less than 2 μm) and fine mode ($D_p < 1.13$ μm). Fine mode was further subdivided into nuclei ($D_p < 0.1$ μm) and accumulation mode ($0.1 < D_p < 1.13$ μm).

[30] Relative fractions of these three modes, for each observation day, are shown in Figure 6a. It is clear that particle mass, during winter season, is dominated by accumulation mode particles contributing ~71% of the total mass. Coarse mode particles also have significant share of the total particles mass (~25%). The monthly average, mean proportion of each mode and the average values during foggy/hazy and clear days of the three modes are given in Tables 4 and 5. A *t* test has been performed on the average values of mass concentration for each mode to compare the levels during foggy/hazy and clear days. Only accumulation mode particle mass concentration shows large increase (~116%) during foggy/hazy days.

[31] For the modeling of optical properties, particle size distribution is an important input. Thus particle mass distribution model with bimodal lognormal distribution has been fitted. The observed size distribution can be described as sum of two lognormal distributions.

$$n_M(D_p) = \sum_{i=1}^{2} \frac{M_i}{(2\pi)^{1/2} \log \sigma_i} \exp\left(-\frac{\left(\log D_p - \log \overline{D_{pi}}\right)^2}{2\log^2 \sigma_i^2}\right) \quad (5)$$

[32] The mass medium diameters (D_p) are 0.28 and 8 μm, respectively, for fine and coarse modes and log σ (logarithmic geometric standard deviation) are 0.985 and 0.916, respectively. It will be interesting to measure the particle size distribution during premonsoon and monsoon season to see the influence of dust on coarse mode particles.

[33] As compared to M_T measured during LC I in the peninsular India [*Moorthy et al.*, 2005a], M_T in Kanpur is very high. Even in the so-called hot spots in peninsular India, M_T never exceeded 100 μg m^{-3}. However, the proportion of fine and coarse mode particles to M_T was found to be similar in both the regions, which indicates that the nature of aerosol loading (anthropogenic contribution dominating) during the winter season is quite similar, although the magnitude of loading is much higher in northern India as compared to peninsular India.

3.4.2. Particle Number Distribution

[34] Particle number distribution is an important input parameter in calculating the extinction coefficient of aerosols. Smaller particles also pose health hazards to human being. In particular increasing exposure of children to the fossil fuel derived particles is a matter of concern in recent years [*Grigg*, 2002]. Hence it is important to know their distribution.

[35] The total number concentration (N_T) of particles was obtained by summing the numbers in each bin from 0.3 to 20 μm. N_T was found to vary between ~1.5 to 2×10^3 #cm^{-3} with maximum particles concentration during foggy/hazy days. This is also confirmed from the large increase in $\tau_{a,500}$ (Figure 4a). N_T was subdivided in two modes, fine ($0.3 < D_p < 2$ μm, N_f) and coarse ($2 < D_p < 20$ μm, N_c) fractions. The monthly average values of N_T, N_f and N_c, and the average values during

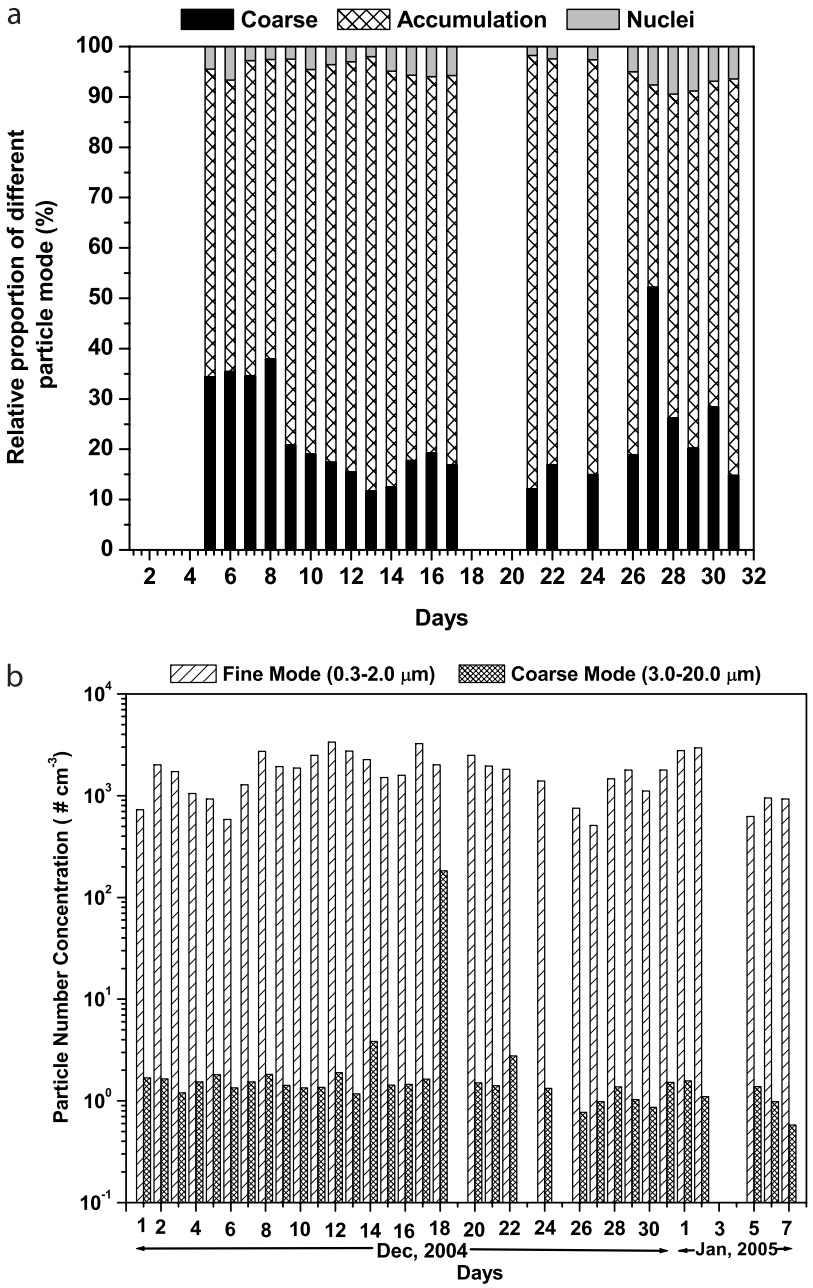

Figure 6. (a) Relative contribution of nuclei, accumulation, and coarse mode particles to the total aerosol mass concentration measured by QCM during December 2004. (b) Relative contribution of fine and coarse mode particles to the total aerosol number concentration measured by OPC during December 2004.

foggy/hazy and clear days are summarized in Tables 4 and 5. Fine mode particles contribute to 99.6%, and the rest being the contribution of coarse mode particles (Figure 6b). Both N_f and N_c show marked increase during foggy/hazy days (53% and 21%, respectively). It is interesting to note that at the coarse mode, the number concentration increases during the foggy period, whereas the mass concentration does not show any statistically significant difference. This is due to the fact that the cutoff diameters for the fine and coarse mode in QCM and OPC measurements are slightly different; as well as the absolute values of number concentration during foggy/hazy (1.7 ± 0.3 particles cm^{-3}) and clear (1.4 ± 0.2 particles cm^{-3}) days are small. Hence an increment of only 0.3 particles cm^{-3} shows significant difference statistically.

[36] The measured particle number distribution during monthly average, clear and foggy/hazy days were fitted as power law distribution, as the measured N_T shows generally decreasing trend with increasing particle size in the range $0.3 < D_p < 20$ μm;

$$n_N(\log D) = {}^{C}\Big/_{(D^V)} \tag{6}$$

Table 4. Statistical Values of Aerosol Mass and Number Concentration at Kanpur During Land Campaign II

Component[a]	Monthly Mean, $\mu g\ m^{-3}$	SD σ	Mean Proportion, %
QCM mass concentration, $\mu g/m^{-3}$			
Nuclei	5.4	2.4	4.7
Accumulation	92.2	42.8	70.4
Coarse	28.4	7.03	24.9
Total	126.0	47.1	
OPC number concentration, cm^{-3}			
Fine mode (0.3–2.0 μm)	1.72×10^3	4.2×10^2	99.6
Coarse mode (2.0–20.0 μm)	1.47	0.27	0.4
Total	1.73×10^3	3.0×10^2	

[a]QCM, quartz crystal microbalance; OPC, optical particle counter.

where C and ν are constants, n_N is the particle number concentration and D is the diameter of the particle. The values of C and α for the whole month, foggy/hazy and clear days are 17 cm^{-3}, 2.72; 48 cm^{-3}, 2.44 and 8.75 cm^{-3}, 3.06, respectively.

[37] The aerosol mass and number size distribution measured by QCM and OPC were for the ambient aerosols. The dry aerosol mass was not measured during the campaign, however, the variation of measured aerosol mass with RH has been considered. Correlation between the hourly averaged mass and the corresponding RH is examined. Accumulation mode particle mass was found to show significant correlation with RH (R = 0.83), whereas the nuclei and coarse mode particles show very poor correlation (R = 0.06 and 0.15, respectively). Overall, M_T shows significant correlation (R = 0.82) with RH, as it is dominated by accumulation mode particles. M_T was found to increase with RH at RH > 27%. The analysis revealed that highly humid conditions in the hazy/foggy period mostly affected the accumulation mode particles; as a consequence, the fine mode AOD showed a significant increase in this period (as discussed earlier). On the other hand, N_f and N_c show moderate (R = 0.4) and poor correlation (R = 0.2) with RH.

3.5. Comparative Analysis of Foggy/Hazy and Clear Days

[38] The principal goal of the research work presented in this and the companion paper was to test the hypothesis that anthropogenic aerosol loading significantly contributes to the prolonged and enhanced foggy/hazy winters in plains of the Ganges basin. Comparative analysis of foggy/hazy and clear day atmospheric parameters and characterization of the aerosols could reveal significant information to partially validate the hypothesis. The percentage deviation of the accumulation and coarse mode particles from the monthly mean during December is shown in Figure 7a. It can be noticed that during fog/haze, the fractional increment was more for the accumulation mode particles followed by coarse mode. Accumulation mode particles generally act as condensation nuclei, which may form fog droplets upon condensation of water vapor. Soluble gases, e.g., HNO_3 and SO_2, dissolve into these fog droplets, and a series of aqueous reactions take place in these droplets. Most prominent among these are conversion of S(IV) to S(VI). The sulfate in S(VI) form is nonvolatile and remains in particulate phase (this result is discussed in detail in the companion paper by *Tare et al.* [2005]). As a result of these aqueous reactions particle mass and size generally increases after the fog processing [*Pandis et al.*, 1990a, 1990b; *Seinfeld and Pandis*, 1998].

[39] Particle mass size distributions are plotted for forenoon (Figure 7b) and afternoon (Figure 7c) averaged for foggy/hazy and clear days. The bimodal nature of particle size distribution is clearly evidenced with enhanced accumulation and coarse mode during foggy/hazy days, which is more pronounced during afternoon. In general particle mass distribution peak increases by a factor of 2 during fog/haze occurrence. The number size distribution also shows similar behavior (Figures 7d and 7e).

[40] The increase in mass concentration during fog was also due to increased stability in the boundary layer, allowing the particles to be concentrated near the surface (refer to Figures 3a–3c). Average diurnal variations of accumulation and coarse mode particle mass for foggy/hazy and clear days are plotted in Figures 8a and 8b. Accumulation mode particle mass shows strong diurnal variation with maxima peak in the morning hours and the mass has an upward slope around 1700 LT. Since the measurement protocol restricted the measurements only till 1700 LT, the peak at 1700 LT is not seen in the figure. However, similar trend has

Table 5. Statistical Values of Aerosol Mass and Number Concentration During Foggy/Hazy and Clear Weather Days at Kanpur

Component	Value on Foggy/Hazy Days	Value on Clear Days	Statistical Inference at 5% Significance[a]
QCM mass concentration, $\mu g/m^3$			
Nuclei mode	5.7 ± 2.3	4.7 ± 2.5	F/N ↔
Accumulation mode	115.9 ± 37.9	53.5 ± 28.0	F/N ↑
Coarse mode	24.2 ± 6.0	24.2 ± 5.6	F/N ↔
AOD	0.9 ± 0.3	0.6 ± 0.2	F/N ↑
OPC number concentration, cm^{-3}			
Fine	$2.0 \times 10^3 \pm 6.9 \times 10^2$	$1.3 \times 10^3 \pm 7.2 \times 10^2$	F/N ↑
Coarse	1.7 ± 0.3	1.4 ± 0.2	F/N ↑

[a]F/N up, foggy/hazy period level is significantly high; F/N down, clear period level is significantly high; F/N even, no significant difference.

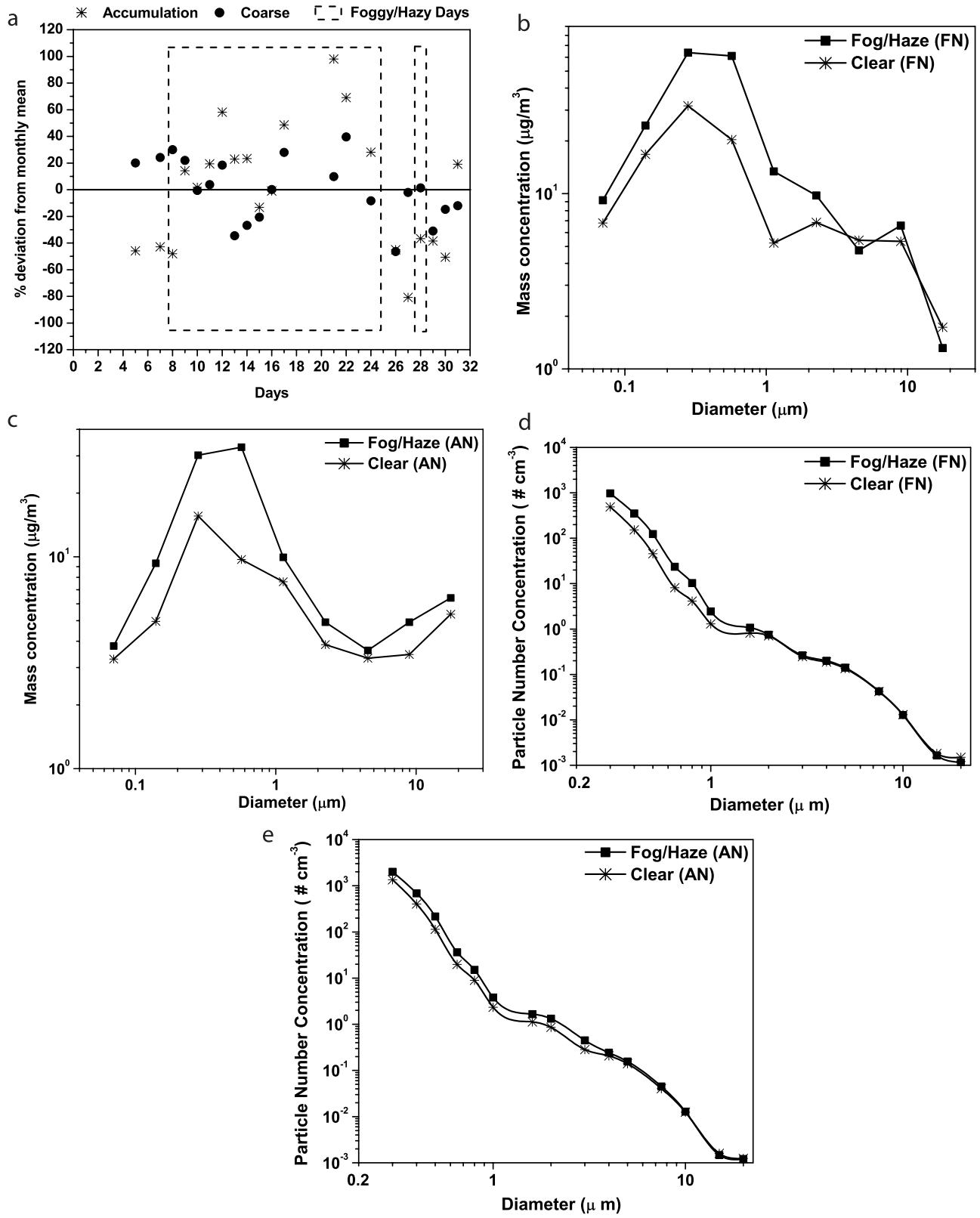

Figure 7. (a) Percentage deviation of mass of accumulation and coarse mode particles from monthly mean value. (b) Aerosol mass size distribution during forenoon of foggy/hazy and clear days. (c) Same as Figure 7b, but during afternoon. (d) Same as Figure 7b, but for aerosol number size distribution. (e) Same as Figure 7d, but during afternoon.

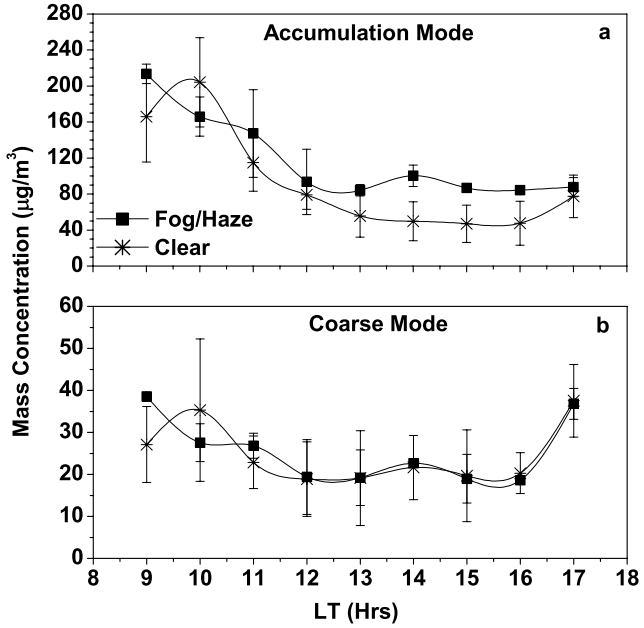

Figure 8. Diurnal variation of (a) accumulation and (b) coarse mode particles during foggy/hazy and clear days.

been observed for aerosol black carbon during December period [*Tripathi et al.*, 2005a] that confirms the strong diurnal trend in aerosol mass. Values as high as 210 μg m^{-3} have been observed during early morning hours, with a slight shift in the peak toward the left during foggy/hazy days. The difference between aerosol accumulation mode concentration between foggy/hazy and clear days can be explained from the difference between diurnal variations of temperature and RH during the two periods. Similar diurnal variation was observed for coarse mode particles, but here the difference diminishes after the morning hours.

4. Conclusions

[41] Atmospheric and aerosol parameters from a typical location in the Ganga basin in Northern India measured during a comprehensive field campaign in the winter season (December 2004) are presented. The major conclusions may be stated as follows:

[42] 1. Aerosol optical and physical properties show marked differences during foggy/hazy and clear conditions; aerosol mass and number concentration are significantly higher during the foggy/hazy days because of the existence of stable shallow boundary layer and plausible contribution to pollutant loads due to anthropogenic activities. This is reflected in the significant increase in fine mode AOD (due to increase mostly in accumulation mode particles) and higher curvature in the AOD spectrum during the hazy/foggy period.

[43] 2. Monthly averaged AOD is quite high (0.77) and shows high spectral variation. The spectral dependence of $\omega_{0,dry}$ is higher than that of the ambient aerosols because of higher rate of change of SSA with RH ($\Delta\omega_0/\Delta$RH) at higher wavelengths. The decreasing trend of SSA with wavelength reveals dominant mixing of absorbing BC with nonabsorbing components for most of the time. Although, statistically, the mean R_{eff} for the clear days (0.71 ± 0.14) is not much different from the corresponding mean for hazy/foggy days (0.76 ± 0.1), the diurnal variation of R_{eff} is much lower in the hazy/foggy period as compared to that during the clear days.

[44] 3. Aerosol mass concentration varies in the range 45 to 220 μg m^{-3} with a monthly mean of 125.9 ± 47.1 μg m^{-3}. Accumulation mode particles contribute 71%, coarse mode 25% and nuclei mode the rest to the total mass concentration. Aerosol mass size distribution is represented as lognormal bimodal distribution, whereas the number size distribution is fitted with inverse power law distribution. Fine mode particles contribute to 99.6% to the observed total number concentration.

[45] **Acknowledgments.** This work is carried out under the Indian Space Research Organization's Geosphere Biosphere Programme Land Campaign II. The efforts of PIs in establishing and maintaining the IIT Kanpur AERONET site are highly appreciated. S.N.T. acknowledges helpful discussion with Chandra Venkataraman.

References

Ackerman, A. S., O. B. Toon, D. E. Stevens, A. J. Heymsfield, V. Ramanathan, and E. J. Welton (2000), Reduction of tropical cloudiness by soot, *Science*, *288*, 1042–1047.

Ångström, A. (1964), The parameters of atmospheric turbidity, *Tellus*, *16*, 64–75.

Bates, T. S., B. J. Huebert, J. L. Gras, F. B. Griffiths, and P. A. Durkee (1998), International Global Atmospheric Chemistry (IGAC) Project's First Aerosol Characterization Experiment (ACE 1): Overview, *J. Geophys. Res.*, *103*, 16,297–16,318.

Bergstrom, R. W., P. B. Russell, and P. Hignett (2002), On the wavelength dependence of absorption of black carbon particles: Predictions and results from the TARFOX experiment and implications for the aerosol single scattering albedo, *J. Atmos. Sci.*, *59*, 567–577.

Charlson, R. J., S. E. Schwartz, J. M. Hales, R. D. Cess, J. A. Coakley, J. E. Hansen, and D. J. Hoffmann (1992), Climate forcing by anthropogenic aerosols, *Science*, *255*, 423–430.

Chu, D. A., Y. J. Kaufman, G. Zibordi, J. D. Chern, J. Mao, C. Li, and B. N. Holben (2003), Global monitoring of air pollution over land from the Earth Observing System–Terra Moderate Resolution Imaging Spectroradiometer (MODIS), *J. Geophys. Res.*, *108*(D21), 4661, doi:10.1029/2002JD003179.

Cros, B., et al. (2004), The ESCOMPTE program: An overview, *Atmos. Res.*, *69*, 241–279.

Dey, S., S. N. Tripathi, R. P. Singh, and B. N. Holben (2004), Influence of dust storms on aerosol optical properties over the Indo-Gangetic basin, *J. Geophys. Res.*, *109*, D20211, doi:10.1029/2004JD004924.

Dey, S., S. N. Tripathi, R. P. Singh, and B. N. Holben (2005), Seasonal variability of the aerosol parameters over Kanpur, an urban site in the Indo-Gangetic basin, *Adv. Space Res.*, *36*, 778–782.

Dey, S., S. N. Tripathi, R. P. Singh, and B. N. Holben (2006), Retrieval of black carbon and specific absorption over Kanpur city, northern India during 2001–2003 using AERONET data, *Atmos. Environ.*, *40*, 445–456.

Dubovik, O., A. Smirnov, B. N. Holben, M. D. King, Y. J. Kaufman, T. F. Eck, and I. Slutsker (2000), Accuracy assessments of aerosol optical properties retrieved from Aerosol Robotic Network (AERONET) Sun and sky radiance measurements, *J. Geophys. Res.*, *105*, 9791–9806.

Dubovik, O., B. N. Holben, T. F. Eck, A. Smirnov, Y. J. Kaufman, M. D. King, D. Tanre, and I. Slutsker (2002), Variability of absorption and optical properties of key aerosol types observed in worldwide locations, *J. Atmos. Sci.*, *59*, 590–608.

Eck, T. F., B. N. Holben, J. S. Reid, O. Dubovik, A. Smirnov, N. T. O'Neill, I. Slutsker, and S. Kinne (1999), Wavelength dependence of the optical depth of biomass burning, urban, and desert dust aerosols, *J. Geophys. Res.*, *104*, 31,333–31,349.

Girolamo, L. D., et al. (2004), Analysis of Multi-angle Imaging Spectroradiometer (MISR) aerosol optical depths over greater India during winter 2001–2004, *Geophys. Res. Lett.*, *31*, L23115, doi:10.1029/2004GL021273.

Goloub, P., J. L. Deuze, M. Herman, D. Tanré, I. Chiapello, B. Roger, and R. P. Singh (2001), Aerosol remote sensing over land using the spaceborne polarimeter POLDER, in *Current Problems in Atmospheric Radiation*, edited by W. L. Smith, and Y. M. Timofeyev, pp. 113–116, A. Deepak, Hampton, Va.

Grigg, J. (2002), The health effects of fossil fuel derived particles, *Arch. Dis. Child.*, *86*(2), 79–83.

Hobbs, P. V., J. S. Reid, R. A. Kotchenruther, R. J. Ferek, and R. Weiss (1997), Direct radiative forcing by smoke from biomass burning, *Science*, *275*, 1776–1778.

Holben, B. N., et al. (1998), AERONET: A federated instrument network and data archive for aerosol characterization, *Remote Sens. Environ.*, *66*, 1–16.

Holben, B. N., et al. (2001), An emerging ground-based aerosol climatology: Aerosol optical depth from AERONET, *J. Geophys. Res.*, *106*, 12,067–12,097.

Huebert, B. J., T. Bates, P. B. Russell, G. Y. Shi, Y. J. Kim, K. Kawamura, G. Carmichael, and T. Nakajima (2003), An overview of ACE-Asia: Strategies for quantifying the relationships between Asian aerosols and their climatic impacts, *J. Geophys. Res.*, *108*(D23), 8633, doi:10.1029/2003JD003550.

Intergovernmental Panel on Climate Change (2001), *Climate Change 2001: The Scientific Basis, Contribution of Working Group I to the Third Assessment Report of the Intergovernmental Panel on Climate Change*, edited by J. T. Houghton et al., 881 pp., Cambridge Univ. Press, New York.

Jacobson, M. Z. (2001), Strong radiative heating due to mixing state of black carbon on atmospheric aerosols, *Nature*, *409*, 695–697.

Jayaraman, A., D. Lubin, S. Ramachandran, V. Ramanathan, E. Woodbridge, W. D. Collins, and K. S. Zalpuri (1998), Direct observations of aerosol radiative forcing over the tropical Indian Ocean during the January-February pre-INDOEX cruise, *J. Geophys. Res.*, *103*, 13,827–13,836.

Kaufman, Y. J., et al. (1998), Smoke, Clouds, and Radiation–Brazil (SCAR-B) experiment, *J. Geophys. Res.*, *103*, 31,783–31,808.

Kiehl, J. T., and B. P. Briegleb (1993), The relative roles of sulfate aerosols and greenhouse gases in climate forcing, *Science*, *260*, 311–314.

Mönkkonen, P., R. Uma, D. Srinivasan, I. K. Koponen, K. E. J. Lehtinen, K. Hameri, R. Suresh, V. P. Sharma, and M. Kulmala (2004), Relationship and variations of aerosol number and PM_{10} mass concentrations in a highly polluted urban environment: New Delhi, India, *Atmos. Environ.*, *38*, 425–433.

Moorthy, K. K., K. Niranjan, B. Narasimhamurthy, V. V. Agashe, and B. V. K. Murthy (1999), Aerosol climatology over India, *ISRO-GBP Sci. Rep. 03-99*, Indian Space Res. Organ., Bangalore.

Moorthy, K. K., et al. (2005a), Wintertime spatial characteristics of boundary layer aerosols over peninsular India, *J. Geophys. Res.*, *110*, D08207, doi:10.1029/2004JD005520.

Moorthy, K. K., S. S. Babu, and S. K. Satheesh (2005b), Aerosol characteristics and radiative impacts over the Arabian Sea during the intermonsoon season: Results from ARMEX field campaign, *J. Atmos. Sci.*, *62*, 192–206.

O'Neill, N. T., T. F. Eck, A. Smirnov, B. N. Holben, and S. Thulasiraman (2003), Spectral discrimination of coarse and fine mode optical depth, *J. Geophys. Res.*, *108*(D17), 4559, doi:10.1029/2002JD002975.

Pandis, S. N., J. H. Seinfeld, and C. Pilinis (1990a), Chemical composition differences among droplets of different sizes, *Atmos. Environ., Part A*, *24*, 1957–1969.

Pandis, S. N., J. H. Seinfeld, and C. Pilinis (1990b), The smog-fog-smog cycle and acid deposition, *J. Geophys. Res.*, *95*, 18,489–18,500.

Pasricha, P. K., B. S. Gera, S. Shastri, H. K. Maini, A. B. Ghosh, M. K. Tiwari, and S. C. Garg (2003), Role of the water vapor greenhouse effect in the forecasting of fog occurrence, *Boundary Layer Meteorol.*, *107*(2), 469–482.

Penner, J. E., et al. (2001), Aerosols, their direct and indirect effects, in *Climate Change 2001: The Scientific Basis: Contribution of Working Group I to the Third Assessment Report of the Intergovernmental Panel on Climate Change*, edited by J. T. Houghton et al., pp. 291–348, Cambridge Univ. Press, New York.

Pillai, P. S., and K. K. Moorthy (2001), Aerosol mass size distributions at a tropical coastal environment: Response to mesoscale and synoptic processes, *Atmos. Environ.*, *35*, 4099–4112.

Raes, F., T. Bates, F. McGovern, and M. VanLiedekerke (2000), The 2nd Aerosol Characterization Experiment (ACE-2): General overview and main results, *Tellus, Ser. B*, *52*, 111–125.

Ramanathan, V., and M. V. Ramana (2005), Persistent, widespread, and strongly absorbing haze over the Himalayan foothills and the Indo-Gangetic plains, *Pure Appl. Geophys.*, *162*, 1609–1626.

Ramanathan, V., et al. (2001), Indian Ocean Experiment: An integrated analysis of the climate forcing and effects of the great Indo-Asian haze, *J. Geophys. Res.*, *106*, 28,371–28,398.

Russell, P. B., J. M. Livingston, P. Hignett, S. Kinne, J. Wong, A. Chien, R. Bergstrom, P. Durkee, and P. V. Hobbs (1999), Aerosol-induced radiative flux changes off the United States mid-Atlantic coast: Comparison of values calculated from sunphotometer and in situ data with those measured by airborne pyranometer, *J. Geophys. Res.*, *104*, 2289–2307.

Satheesh, S. K., and V. Ramanathan (2000), Large differences in tropical aerosol forcing at the top of the atmosphere and Earth's surface, *Nature*, *405*, 60–63.

Seinfeld, J. H., and S. N. Pandis (1998), *Atmospheric Chemistry and Physics*, pp. 812–823, John Wiley, Hoboken, N. J.

Singh, R. P., S. Dey, S. N. Tripathi, V. Tare, and B. N. Holben (2004), Variability of aerosol parameters over Kanpur, northern India, *J. Geophys. Res.*, *109*, D23206, doi:10.1029/2004JD004966.

Tare, V., et al. (2005), Measurements of atmospheric parameters during ISRO-GBP Land Campaign II at a typical location in Ganga basin: 2. Chemical properties, *J. Geophys. Res.*, *111*, D23210, doi:10.1029/2006JD007279.

Tiwary, A., and J. J. Colls (2004), Measurements of atmospheric aerosol size distributions by collocated optical particles, *J. Environ. Monit.*, *6*, 734–739.

Tripathi, S. N., S. Dey, V. Tare, and S. K. Satheesh (2005a), Aerosol black carbon radiative forcing at an industrial city in northern India, *Geophys. Res. Lett.*, *32*, L08802, doi:10.1029/2005GL022515.

Tripathi, S. N., S. Dey, V. Tare, S. K. Satheesh, S. Lal, and S. Venkataramani (2005b), Enhanced layer of black carbon in a north Indian industrial city, *Geophys. Res. Lett.*, *32*, L12802, doi:10.1029/2005GL022564.

Twomey, S. (1977), The influence of pollution on the shortwave albedo of clouds, *J. Atmos. Sci.*, *34*, 1149–1152.

Venkataraman, C., G. Habib, A. Figuren-Fernandez, A. H. Miguel, and S. K. Friedlander (2005), Residential biofuels in south Asia: Carbonaceous aerosol emissions and climate impacts, *Science*, *307*, 1454–1456.

A. Agarwal, S. S. S. Chauhan, N. Chinnam, S. Dey, V. P. Kanwade, S. Kishore, R. B. Lal, M. Manar, M. Sharma, A. K. Srivastava, V. Tare, and S. N. Tripathi, Department of Civil Engineering, Indian Institute of Technology, Kanpur-208016, India. (snt@iitk.ac.in)

K. R. Gopal, K. Narasimhulu, L. S. S. Reddy, and R. R. Reddy, Department of Physics, Sri Krishnadevaraya University, Andhra Pradesh, Sri Venkateswarapuram, Anantapur-515003, India.

S. Gupta and S. Lal, Physical Research Laboratory, Ahmedabad -380009, India.